

## Microstructure evolution of amorphous-ZrCuNiAlSi/Ag composite

LL Miao <sup>1)</sup>, F Wang <sup>2)</sup>, P Huang <sup>3)</sup>

<sup>1), 3)</sup> *State-key Laboratory for Mechanical Behavior of Material, Xi'an Jiaotong University, Xi'an, 710049, China.*

<sup>2)</sup> *State-Key Laboratory for Strength and Vibration of Mechanical Structures, School of Aerospace, Xian Jiaotong University, Xi'an, 710049, China.*

[wangfei@mail.xjtu.edu.cn](mailto:wangfei@mail.xjtu.edu.cn)

### Abstract

In this paper, amorphous-ZrCuNiAlSi/crystalline-Ag composites films were fabricated by co-sputtering. The microstructures of these composites were investigated and the hardness was evaluated by nanoindentation in room temperature and shear bands were analyzed. It is found that the hardness of all the composites is higher than that predicted by mixture rule. Besides, the number of shear bands increases to a maximum value of six when the film contain 13.41at% Ag crystalline. The Ag content has a significant influence on mechanical properties, and the addition of Ag atoms can decrease the free volume fraction and the shear transformation zone volume which both have great impact on the hardness and the plasticity of the metallic glasses. The interaction among the soft Ag content, free volume fraction, shear transformation zone volume and interface leads to an optimum value of the hardness and plasticity metallic glasses composites.

Keywords: Nanoindentation, Shear bands, Metallic glasses, Co-sputtering, Composites

---

<sup>1)</sup> Graduate Student

<sup>2)</sup> Associate Professor

<sup>3)</sup> Professor

## **1. INTRODUCTION**

Metallic glass has been thought to be a promising material because of its large elastic module, high strength and excellent corrosion resistance due to the disordered microstructural features without grain boundaries and dislocations (Inoue 2000; Schuh 2007; Spaepen 1976). But the brittleness of metallic glasses is one of the primary factors impeding their adoption in structural applications, as the frequent propagations of shear band (SB) which begins with the aggregation and nucleation of the shear transformation zone (STZ) could dramatically reduce the ductility of metallic glasses (Greer 2013; Homer 2014) .

Numerous studies have concerned on improving the ductility of metallic glasses by the way of adding crystalline layers inside metallic glass, i.e., amorphous/crystal multilayers (Kim 2011; Liu 2013; Wang 2007; Zhang 2012) , porous structure (Brothers 2005) and metallic composites (Hofmann 2008; Jeon 2013; Pauly 2010). By introducing second phase into metallic glass, the multilayer and composite structures were found to be effective ways to restrict SB propagation and eventually to prevent sudden fracture in metallic glasses. Different methods have been introduced to make crystalline-doped microstructure(Eckert 2007), such as addition of insoluble particles to the powder or melt consolidation, annealing, sever deformation and even co-sputtering. Compared to the methods before, co-sputtering is much more convenient for one-step job. But how the different ratios of the amorphous and nanocrystalline will influence the mechanical property is still an unknown question.

It is well known that ductile enhancement of metallic glasses composites are brought by the soft phase, however, the other changes brought by the soft phase which may also change the mechanical properties such as plasticity was not reviewed before.

In this paper, we selected amorphous ZrCuNiAlSi, which has relatively high glass formation ability, to be the amorphous matrix while the soft nanocrystalline Ag to be the second phase to study the influence of the nanocrystalline content and morphology on mechanical property. Except the Ag content, the followed change of STZ volume, free volume fraction and interfaces will be discussed in detail.

## **2. EXPERIMENTAL PROCEDURE**

### *2.1 Specimen preparation*

Monolithic ZrCuNiAlSi film and silver-doped ZrCuNiAlSi (ZrCuNiAlSi/Ag) films with thickness of ~1500nm were deposited on single Si (1 1 1) substrate at room temperature by means of magnetron sputtering with ZrCuNiAlSi and Ag (purity > 99.99) target. The direct current (DC) sputtering power applied for ZrCuNiAlSi target was 100W,

and the radio frequency (RF) sputtering power applied for Ag target was changed from 10W to 40W. By using energy-dispersive X-ray spectrometer (EDS) analysis, the content of Ag was estimated to be 5.07at%, 13.41at%, 33.14at% and 33.37at% for the samples deposited at 10W, 15W, 30W and 40W, respectively. The ZrCuNiAlSi/Ag film that deposited at 10W, as an example, was referred to Zr-based/Ag-10W hereafter, and the other three composites follows the identical terminology. Before deposition, 15 minutes pre-sputtering was conducted to clean the target surface, and the vacuum background pressure was less than  $5.0 \times 10^{-4}$  Pa. The microstructure of the films were determined by high-resolution transmission electron microscope (HRTEM, JEM2100F) operating at 200KV.

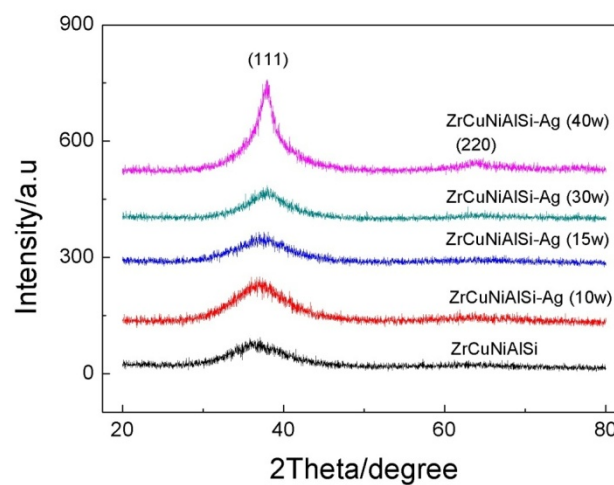


Fig.1 XRD patterns of ZrCuNiAlSi and the ZrCuNiAlSi/Ag composites

## 2.2 Indentation testing

The mechanical properties of the composite films were conducted by nanoindentation tests which were performed using a dynamic contact module device equipped within Nanoindenter XP system (MTS, Inc.), under continuous stiffness measurement (CSM) mode at room temperature. Upon calibration on standard fused silicon, the tip of the Berkovich diamond indenter was estimated to have a radius of ~150 nm.

The hardness of the composite samples was examined by depth control mode at loading strain rate (LSR) of  $0.05 \text{ s}^{-1}$ . At least 12 indents were made on each sample to minimize result deviation. In loading regime, hardness was automatically recorded as a continuous function of penetration depth by the CSM mode, with the ultimate hardness calculated by averaging the values of the hardness obtained within a certain depth range. In addition, the substrate effect was negligible, since the maximum depth was smaller than  $1/7$  of the film thickness. In addition, the morphologies of the residual

indentations for both the monophase MG and the composites were examined by scanning electron microscopy (SEM).

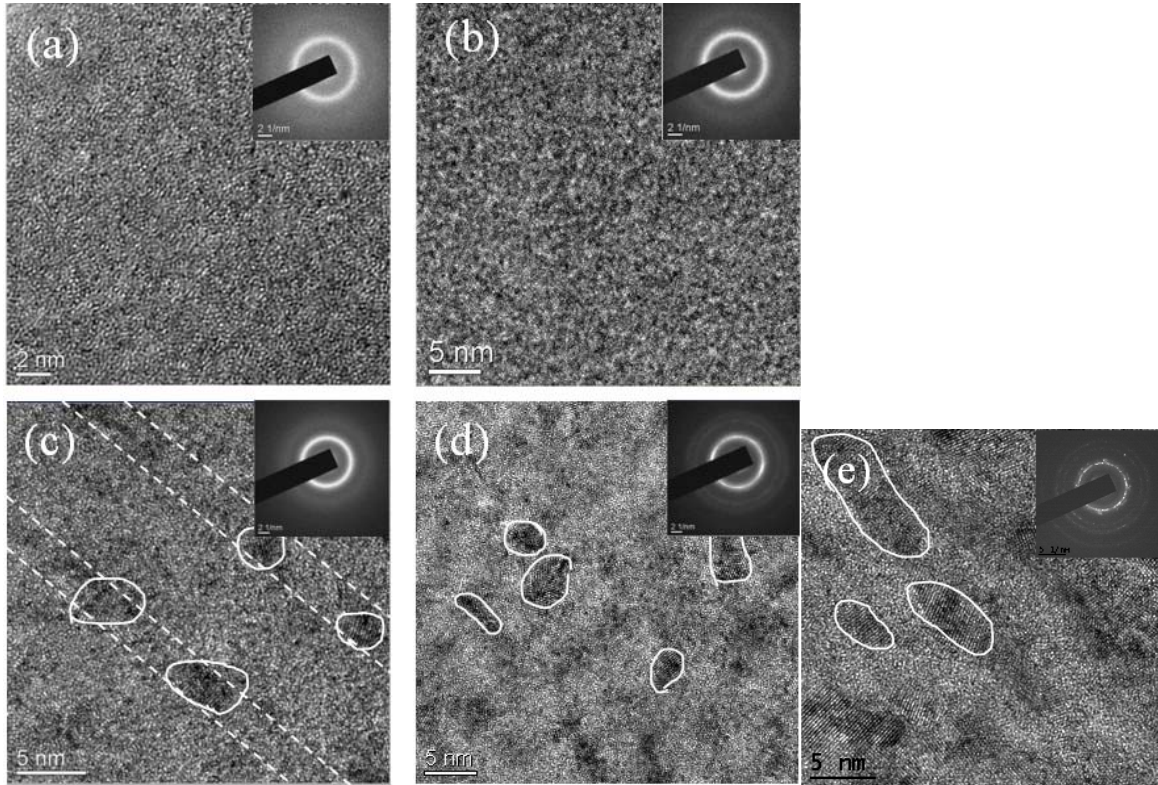


Fig.2 HRTEM of cross-section images of (a) ZrCuNiAlSi amorphous film, (b) ZrCuNiAlSi/Ag (10W), (c) ZrCuNiAlSi/Ag (15W), (d) ZrCuNiAlSi/Ag (30W), (e) ZrCuNiAlSi/Ag (40W)

### 2.3 data analysis

Active volume, of the amorphous ZrCuNiAlSi, ZrCuNiAlSi/Ag composites were evaluated by nanoindentation testing as described in ref. (Choi 2012; Mason 2006). Here, O&P method, was applied and 64 indents were made for each specimen. The initial part of the load-displacement curves were fitted by the Hertzian elastic equation:

$$P = \frac{4}{3} E_r \sqrt{\rho h^3} \quad (1)$$

where  $\rho$  is the effective radius of the Berkovich diamond tip about 50nm, h is the displacement, and  $E_r$  is the reduced modulus

. In addition, the cumulative fraction of the load at the first burst point, F could be expressed as:

$$\ln[-\ln(1-F)] = \frac{0.47}{\pi} \left( \frac{4E_r}{3\rho} \right)^{2/3} \frac{V^*}{kT} P^{1/3} + \beta \quad (2)$$

where  $\beta$  is a constant that depend on load P, T is environment temperature,  $V^*$  is the volume of the event which is equal to the free volume. Then the slope of the curve that  $\ln[-\ln(1-F)]$  vs. P, which is proportional to  $V^*$ , could be derived.

### 3. RESULTS AND DISCUSSION

#### 3.1 Microstructure

High Resolution Transmission Electron Microscopy (HRTEM) image shown in Fig. 1(a) revealed the typical maze microstructure of the monophase Zr-based MG film. Figure 2 showed the HRTEM cross-sectional images of the ZrCuNiAlSi/Ag composites. No obvious crystalline phase was observed in Zr-base/Ag-10W with Ag content of 5.07at% as shown in Fig. 2(a), implying it is nearly fully amorphous structure. As the Ag content increased to 13.41at% for Zr-based/Ag-15W, NC Ag regions in length scale of ~2nm were identified within the composites as shown in Fig. 2(b). Further increasing the content of Ag to 31.14at% (Zr-based/Ag-30W) and 33.37at% (Zr-based/Ag-40W), the proportion of NC regions continuously increases and the length scale of the crystalline regions changed to about 5nm as indicated in Figs. 2(c) and 2(d). The tendency that the fraction volume of the crystalline regions increases at higher sputtering power was confirmed by the inserted SAD patterns shown in Fig. 2, since the intensities of the diffraction spots and the diffraction rings corresponding to crystalline structure gradually increased as sputtering power increases.

#### 3.2 Mechanical properties

In this section, the effects of the microstructure and the different crystalline Ag contents on the mechanical properties upon nanoindentation were provided and discussed.

##### 3.2.1 Hardness

To demonstrate the effects, first of all, the hardness was plotted as a function of crystalline Ag content in Fig. 3, compared with the red line which was derived from the rule of mixture (ROM):

$$\sigma_{ROM} = \sigma_{MG}(1 - f) + \sigma_{Ag}f \quad (5)$$

where  $f$  is the volume fraction of Ag in the composites. Clearly, the hardness derived via indentation testing is higher than that calculated by ROM model. In addition, the hardness of the composites increases slightly for the Zr-based/Ag-10W with crystalline Ag content of ~5.07at%, compared with the monolithic Zr-based MG film. Then, the hardness decrease continuously as crystalline Ag content increases, even though all the values of hardness for the other three composites are larger than that predicted by ROM model. The residual indentation at penetration depth of 800nm was observed under the Scanning Electron Microscope (SEM) as shown in Fig 2(b).

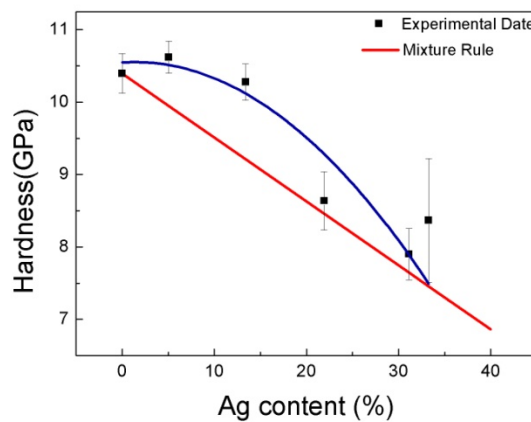


Fig.3 Hardness as a function of Ag content in ZrCuNiAlSi/Ag composites.

Figure 4 presents SEM images of the residual indentations at penetration depth of 800nm composite ZrCuNiAlSi films, and multiple SBs were observed. As shown in Fig. 6, the number of SBs in the composite films increases initially with the crystalline Ag content, and subsequently decreases after reaching a maximum value of ~6 at 13.41at% Ag for Zr-based/Ag-15W. In the following, we will discuss how the crystalline content, morphology will impact on the hardness and the microstructural deformation mechanism under nanoindentation.

### 3.2.2 Shear banding deformation

Keeping on increasing the Ag content to 13.41at%, obvious Ag crystalline the number of the shear bands raises to 6 and the shear band space  $\omega$  is very narrow. There are two main reasons for this: (I) the emerged ductile nanocrystalline provided more nucleation sites for shear bands due to stress-strain differences in these two phases and act as microstructural arrest barriers to shear band propagation which

leading to wave shear bands (Abdeljawad 2011); (II), the phenomena that the crystal concentrated in narrow band (Fig. 3(c)) can prevent the propagation of the shear bands more effectively, meanwhile, this is the reason of small  $\omega$ . But as the Ag content continues ascending, the shear bands decreases again. With the addition of Ag, the shear bands decrease due to the reason that soft Ag can undertake part of the plastic deformation, The crystal/amorphous interfaces also increase along with the increase of Ag content and play a more important role in plastic deformation. The deformation mechanism become interface dominated deformation from shear band dominated deformation.

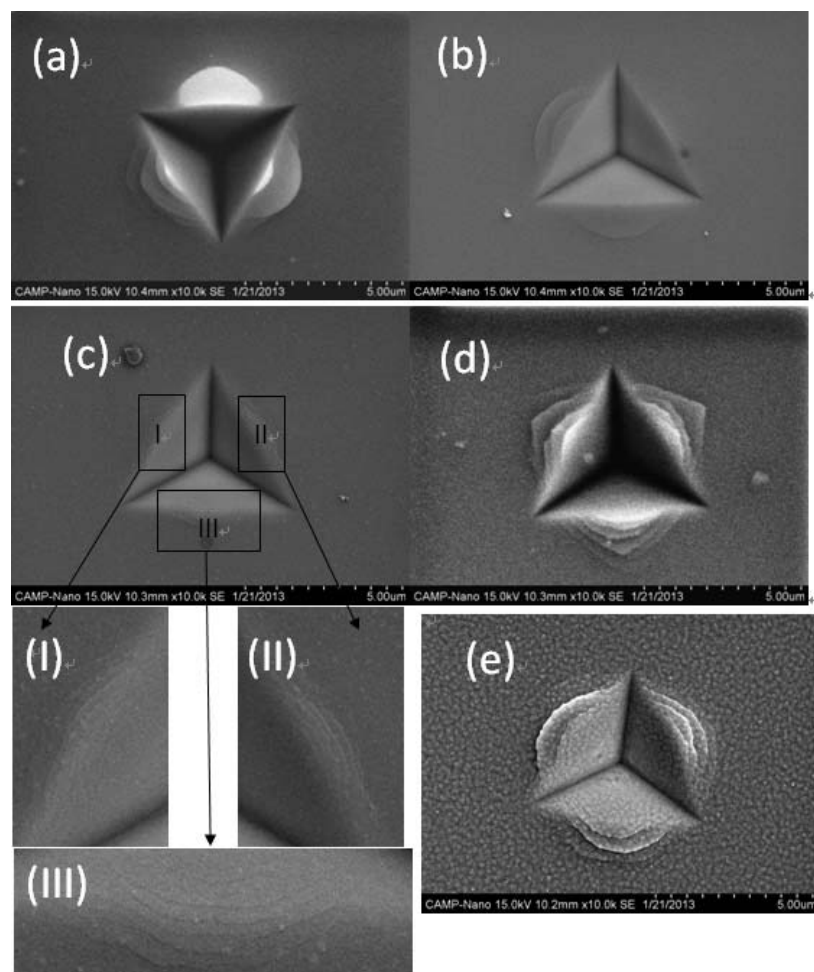


Fig.4 SEM images showing indents in (a) ZrCuNiAlSi film, (b) ZrCuNiAlSi/Ag(10w), (c) ZrCuNiAlSi/Ag(15w), (d) ZrCuNiAlSi/Ag(30w), (f) ZrCuNiAlSi/Ag(40w) and (I) (II) (III) show the local amplificatory figures corresponding to (c).

The Ag content below 15at%, the hardness and plasticity are both abnormal compared with the overall trend. Free volume (FV) changed by the Ag atoms may play a more important role here.

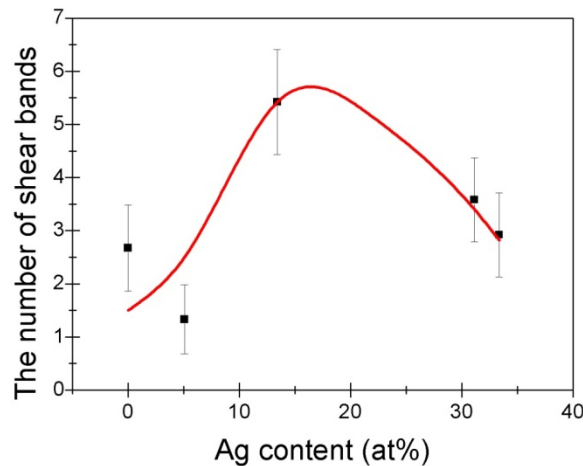


Fig.5 The number of shear bands as a function of the Ag content.

Due to a handful of Ag atoms in the metallic glasses do not form nanocrystalline, but form Ag-ZrCuNiAlSi amorphous alloy (as shown in Fig. 2 (a)) can change the fraction and the concentration of the free volume fraction of metallic glass (Xu 2010). the radius of Ag atom is 0.118nm which is between the Cu (0.145nm), Al (0.118nm), Ni (0.124nm) and Zr (0.206nm) which will lead to the increase the atom packing density which means the fraction of the free volume will decrease; while the medium-range ordered (IMO) structure may make the FV concentrated around the IMO cluster (Ren 2011). According to this, the free volume of Ag-ZrCuNiAlSi amorphous alloy may be lower than ZrCuNiAlSi. Numerous reports have researched the how the FV impact the mechanical properties through annealing, and the results shows the decrease of FV will cause the increase of the hardness (Gu 2013). Fig. 6 shows HRTEM analysis of FV in the composites samples of Zr-MG, Zr-MG-Ag (10W) and Zr-MG-Ag (15W). Herein, the methods was developed by Miller and Gibson, later extended by Li (Li 2002), Jiang (Jiang 2003) and Zhu (Zhu 2011), was adopted. Fig. 6a-c corresponds to the converted images for the Zr-MG, Zr-MG-Ag (10W) and Zr-MG-Ag (15W) respectively. In accordance, as shown in Fig. 6d-f, the bright part represents the zone with less FV. The conventional TEM contrast comes mainly from the specimen mass thickness; hence, it is readily shown that, with increasing Ag content, less FV is concentrated in a certain zone. With Ag content increased, the obvious Ag crystal emerged, which cause hardness decreasing slightly, and then are according with the ROM gradually. This is result of the competition between the hardness increase caused by the decrease of the FV and the hardness decrease caused by the addition of soft Ag.

The first three samples (ZrCuNiAlSi, ZrCuNiAlSi/Ag (10W) and ZrCuNiAlSi/Ag (15W)) are also been evaluated the active volume which determined the STZ volume. The results show in Table 1 that the activation volume which is in direct proportion to

STZ volume becomes smaller as the Ag content bigger and the small STZ volume will promote the multi shear bands (Liu 2012).

Table 1 The activation volume of the Zr-based thin films

Sample	Am	Am-Ag(10W)	Am-Ag(15W)
Activation volume $V^*$ (nm <sup>3</sup> )	0.0213	0.0162	0.0147

The effects of the crystalline Ag content the evolution and propagation of shear bands was examined in the following. Previously, computer simulations have indicated that large nanocrystals with grain size as large as twice the thickness of shear band could effectively interact with nascent shear bands (Lund 2007). In addition, Lund et al also demonstrated that crystalline inclusions could also affect the stress field in the glassy matrix. Not only the grain size is of importance but also the grain shape.

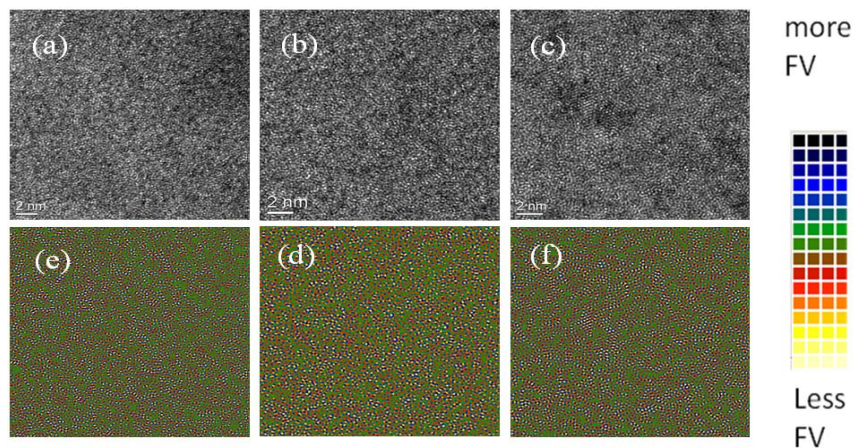


Fig.6 HRTEM images for (a) ZrCuNiAlSi amorphous film, (b) ZrCuNiAlSi/Ag (10W), (c) ZrCuNiAlSi/Ag (15W). (d), (e) and (f) Fourier-filtered, threshold filtered and inverted images corresponding to (a), (b) and (c), respectively.

### 3.3 Effects of crystalline-amorphous interface

Figure 2 can observed clear interfaces between amorphous and crystalline region without defined orientation relationship between the two phases because of the disordered structure of the metallic glass. The role of amorphous-crystalline interfaces (ACIs) has been research in multilayers (Brandl 2013; Wang 2007). The simulation proved that the deformation of ACIs and showed that the ACI sliding which is similar to GB sliding will promote the deformation of films. During deformation, the Ag crystalline yields and alters not only its own geometry but also the adjacent amorphous metals through the interfaces. Interfaces can not only absorb part of the stress caused by the

deformation of Ag region, but also can stimulate STZs of amorphous metal; on the contrary, interfaces can also dissipate energy of shear bands. At a critical level, the STZs will nuclear and form shear bands. In reverse, the shear bands propagation can be deflected or stopped by the ACIs. Hence, the soft Ag region governing the deformation first in the amorphous composites, then, the stress and strain transfer to the amorphous part through ACIs. Increasing the strain, the interface and amorphous metal will be spontaneous deformation instead of being stimulated. Thereby, the increased interfaces can undertake part of the deformation and improve the plasticity.

Table 2 Summary of the roles of the various factors influenced the mechanical properties.

Influence factor	mechanism	Contribution to strength	Contribution to plasticity
Crystalline	Intrinsic properties	Soften	strengthen
	Deflection and branching of shear bands	Strengthen	strengthen
STZ volume	The site for SB nucleation		strengthen
Free volume	Atomic stacking	Strengthen/high	soften
Interface	ACIs sliding and load transfer	Strengthen	strengthen

It is noted that, the hardness of the stripped crystalline embedded one is higher due to the stripped crystalline will introduce more stress concentration. Overall, we are able to conclude that the composite structure can enhance the hardness. The main factors and the contribution were summarized in Table 2.

#### 4. CONCLUSION

The mechanical properties of Zr-based amorphous alloys with different fraction and morphology have been investigated. The composites have a higher hardness than that of ROM, especially a spot of Ag addition and at this spot, the number of shear band arrive at maximum which indicate a optimum value except the role of the second phase, the

extra atoms addition will decrease the free volume fraction and STZ volume of metallic glasses. Hence, this will enhance hardness and promote multi shear bands respectively.

## ACKNOWLEDGEMENTS

This work was financially supported by the National Natural Science Foundation of China (51171141, 51271141), and the Program for New Century Excellent Talents in University (NCET-11-0431).

## REFERENCES

- Abdeljawad, F., Fontus, M., Haataja, M., (2011), "Ductility of bulk metallic glass composites: Microstructural effects," *Appl. Phys. Lett.* **98** (3), 031909.
- Brandl, C., Germann, T.C., Misra, A., (2013), "Structure and shear deformation of metallic crystalline-amorphous interfaces," *Acta. Mater.*, **61**, 3600-3611.
- Brothers, A.H., Dunand, D.C., (2005), Ductile bulk metallic glass foam. *Adv. Mater.*, **17**, 484-486.
- Choi, I.-C., Zhao, Y., Yoo, B.-G., Kim, Y.-J., Suh, J.-Y., Ramamurty, U., Jang, J.-i., (2012), "Estimation of the shear transformation zone size in a bulk metallic glass through statistical analysis of the first pop-in stresses during spherical nanoindentation," *Scripta. Mater.*, **66** (11), 923-926.
- Eckert, J., Das, J., Pauly, S., Duhamel, C., (2007), "Processing Routes, Microstructure and Mechanical Properties of Metallic Glasses and their Composites," *Adv. Eng. Mater.*, **9** (6), 443-453.
- Greer, A.L., Cheng, Y.Q., Ma, E., (2013), "Shear bands in metallic glasses," *Mater. Sci. Eng.*, **R74** (4), 71-132.
- Gu, J., Song, M., Ni, S., Guo, S., He, Y., (2013), "Effects of annealing on the hardness and elastic modulus of a Cu<sub>36</sub>Zr<sub>48</sub>Al<sub>8</sub>Ag<sub>8</sub> bulk metallic glass," *Mater. Des.*, **47**, 706-710.
- Hofmann, D.C., Suh, J.Y., Wiest, A., Duan, G., Lind, M.L., Demetriou, M.D., Johnson, W.L., (2008), "Designing metallic glass matrix composites with high toughness and tensile ductility," *Nature.*, **451** (7182), 1085-1089.
- Homer, E.R., (2014), "Examining the initial stages of shear localization in amorphous metals," *Acta. Mater.*, **63**, 44-53.
- Inoue, A., (2000), "Stabilization of metallic supercooled liquid and bulk amorphous alloys," *Acta. Mater.*, **48**, 279-306.
- Jeon, C., Kim, C.P., Joo, S.H., Kim, H.S., Lee, S., (2013), "High tensile ductility of Ti-based amorphous matrix composites modified from conventional Ti-6Al-4V titanium alloy," *Acta. Mater.*, **61** (8), 3012-3026.
- Jiang, W.H., Atzmon, M., (2003), "The effect of compression and tension on shear-band structure and nanocrystallization in amorphous Al<sub>90</sub>Fe<sub>5</sub>Gd<sub>5</sub>: a high-resolution transmission electron microscopy study," *Acta. Mater.*, **51** (14), 4095-4105.

- Kim, J.-Y., Jang, D., Greer, J.R., (2011), "Nanolaminates Utilizing Size-Dependent Homogeneous Plasticity of Metallic Glasses," *Adv. Fun. Mater.*, **21** (23), 4550-4554.
- Li, J., Wang, Z., Hufnagel, T., (2002), "Characterization of nanometer-scale defects in metallic glasses by quantitative high-resolution transmission electron microscopy," *Phys. Rev.*, **B65** (14).
- Liu, M.C., Huang, J.C., Fong, Y.T., Ju, S.P., Du, X.H., Pei, H.J., Nieh, T.G., (2013), "Assessing the interfacial strength of an amorphous–crystalline interface," *Acta. Mater.*, **61** (9), 3304-3313.
- Liu, S.T., Wang, Z., Peng, H.L., Yu, H.B., Wang, W.H., (2012), "The activation energy and volume of flow units of metallic glasses," *Scripta. Mater.*, **67** (1), 9-12.
- Lund, A.C., Schuh, C.A., (2007), "Critical length scales for the deformation of amorphous metals containing nanocrystals," *Philos. Mag. Lett.*, **87**, 603-611.
- Mason, J., Lund, A., Schuh, C., (2006), "Determining the activation energy and volume for the onset of plasticity during nanoindentation. *Phys. Rev.*, **B73** (5).
- Pauly, S., Liu, G., Gorantla, S., Wang, G., Kühn, U., Kim, D.H., Eckert, J., (2010), "Criteria for tensile plasticity in Cu–Zr–Al bulk metallic glasses," *Acta. Mater.*, **58** (14), 4883-4890.
- Ren, H.T., Pan, J., Chen, Q., Chan, K.C., Liu, Y., Liu, L., (2011), "Enhancement of plasticity and toughness in monolithic Zr-based bulk metallic glass by heterogeneous microstructure," *Scripta. Mater.*, **64** (7), 609-612.
- Schuh, C., Hufnagel, T., Ramamurty, U., (2007), "Mechanical behavior of amorphous alloys," *Acta. Mater.*, **55** (12), 4067-4109.
- Spaepen, F., (1976), "A microcopuc mechanism for steady state inhomogeneous flow in metallic glasses," *Acta. Mater.*, **25**, 407-415.
- Wang, Y., Li, J., Hamza, A.V., Barbee, T.W., Jr., (2007), "Ductile crystalline-amorphous nanolaminates," *Proc. Natl. Acad. Sci. USA.*, **104** (27), 11155-11160.
- Xu, Y., Zhang, Y., Li, J., Hahn, H., (2010), "Enhanced thermal stability and hardness of Zr<sub>46</sub>Cu<sub>39.2</sub>Ag<sub>7.8</sub>Al<sub>7</sub> bulk metallic glass with Fe addition," *Mater. Sci. Eng.*, **A 527** (6), 1444-1447.
- Zhang, J.Y., Liu, Y., Chen, J., Chen, Y., Liu, G., Zhang, X., Sun, J., (2012), "Mechanical properties of crystalline Cu/Zr and crystal–amorphous Cu/Cu–Zr multilayers," *Mater. Sci. Eng.*, **A 552**, 392-398.
- Zhu, Z.W., Gu, L., Xie, G.Q., Zhang, W., Inoue, A., Zhang, H.F., Hu, Z.Q., (2011), "Relation between icosahedral short-range ordering and plastic deformation in Zr–Nb–Cu–Ni–Al bulk metallic glasses," *Acta. Mater.*, **59** (7), 2814-2822.